

CONTACTLESS ROOM TEMPERATURE CHARACTERIZATION OF PHEMT STRUCTURES USING SURFACE PHOTOVOLTAGE SPECTROSCOPY

M. Leibovitch¹, I. Hallakoun¹, S. Solodky², N. Ashkenasy², G. Bunin¹, Y. Rosenwaks²,

and Yoram Shapira²

¹ELTA Electronics Industries Ltd., P.O.B. 330, Ashdod 77102, Israel, markl@is.elta.co.il, phone 972-8-857-2436

²Department of Physical Electronics, Faculty of Engineering, Tel-Aviv University, Ramat-Aviv 69978, Israel

Abstract

Surface photovoltage spectroscopy has been used for characterization of PHEMT structures. The spectra have been found to be dominated by the electric fields in the structure. These fields are determined by the delta doping levels and by the surface and interface charge densities. A simple empirical model has been developed and used for monitoring changes in the structure growth parameters and surface conditions.

INTRODUCTION

The improved properties of pseudomorphic high electron mobility transistors (PHEMTs) with respect to these of GaAs/AlGaAs high electron mobility transistors have led to intensive integration of the former in the growing market of monolithic microwave integrated circuits. PHEMTs combine the high conductivity of an InGaAs quantum well (QW) layer, which is used as an electron channel, with the properties of wide bandgap AlGaAs layers, which make PHEMT very suitable for high power applications.

The complex design and growth procedures of PHEMTs require an efficient characterization technique to provide information on growth quality and device parameters as early in the procedure as possible. The measurement technique should be contactless, nondestructive, fast, and wafer-scaled. Indeed, photoluminescence (PL)^{1,2}, electroreflectance (ER)^{3,4}, photoreflectance (PR)^{5,6}, X-ray diffraction and reflection⁷ and optical transmission⁸ have been used for the characterization of PHEMT structures.

Information about the energy band-diagram and related fields and charges is essential for probing the device properties. Surface photovoltage spectroscopy (SPS) is a nondestructive, contactless characterization technique, which seems to fulfill these special requirements because of its great sensitivity to electric fields within the structure. SPS monitors changes in the semiconductor surface work function induced by absorption of monochromatic light in the structure, giving rise to surface photovoltage (SPV). A detailed description of this method and its applications may be found in Ref. [9]. Recently, this technique has been successfully applied for the characterization of novel structures and devices such as heterojunction bipolar

transistor,¹⁰ multi-quantum wells,^{11,12} quantum well lasers,¹³ and solar cells¹⁴.

In this work, we apply SPS for the characterization of PHEMT structures. The obtained SPV spectrum is studied both experimentally and numerically. The contribution of different regions of the device to the SPV spectrum is revealed. A simple empirical model has been developed. Two possible applications of this model to estimation of different growth procedure and surface treatments are presented.

SURFACE PHOTOVOLTAGE SPECTROSCOPY OF PHEMT

The SPV spectra have been recorded in air using a commercial Kelvin probe unit (Besocke Delta Phi, Julich, Germany). Illumination is provided through the top layer using a 250 W tungsten-halogen lamp, a grating monochromator (Oriel, USA), and a filter wheel to eliminate second-order harmonics. The measurement sensitivity is about 1 mV, and the light intensity is in the order of 10 $\mu\text{W}/\text{cm}^2$. The measurements were repeated with increased dwell time between repeated monochromator steps in order to ensure steady state conditions during the measurement.

The PHEMT structure is grown on a semi-insulating GaAs wafer with a buffer layer, comprising superlattice and GaAs layers. On it there is a quantum well (QW) channel layer (with a typical In mole fraction of ~20%), sandwiched between the double-sided delta-doped layers (with Si sheet concentration in the range of $1\text{-}5 \times 10^{12} \text{ cm}^{-2}$) and very thin undoped AlGaAs spacers. The top surface layer (also known as the Schottky layer) consists of a thin AlGaAs layer, which separates the channel from the gate electrode, and a highly doped GaAs cap layer, which is used in later process steps for source and drain contact formation.

The SPV effect is due to both charge generation and separation. The latter is governed by the band diagram of the device. The electric fields distribution within PHEMT epist-structure in equilibrium is affected by the doping levels in the delta-doped and cap layers, as well as by interface and surface charges. The redistribution of the carriers within the entire structure determines the device potential distribution, with non-zero electric fields in the buffer, surface and QW regions. Fig 1 shows the band diagram of the structure.

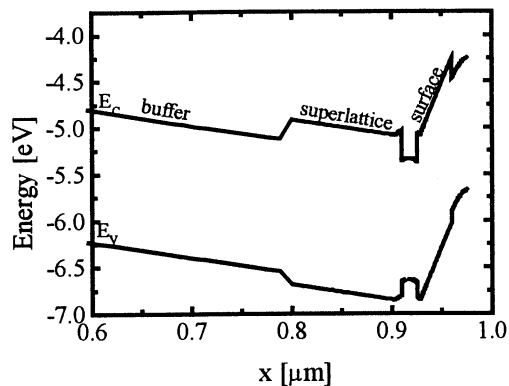


Fig.1 Equilibrium band diagram of a double-sided delta-doped PHEMT structure.

The buffer/substrate interface is designed such that the resultant electric field in the buffer layer (F_B) provides suitable confinement for the hot electrons in the channel under operating conditions. The typical value of the potential drop in the buffer layer is usually of about 1 V ($F_B \sim 15$ kV/cm).

The field in the surface region (F_S) is very sensitive to the conditions at the external surface, and in an actual device, the voltage drop across the Schottky layer may reach 0.7-0.8eV, i.e. $F_S \sim 300$ kV/cm. Thus, in the PHEMT structure, electrons are confined in the vicinity of the well by the buffer and surface fields. On the other hand, the free holes (if they exist) drift away from the QW towards either buffer/substrate or surface interface. Thus, the electron-hole pairs generated by illumination would be separated forming photovoltage (PV) across the structure. Since the directions of the F_B and F_S fields are opposite, the PVs resulting from these regions are of opposite signs. (The PV from the buffer is positive and from the surface it is negative.). Fig 2 shows an actual spectrum of a double delta doped PHEMT structure.

The spectrum contains two peaks: a peak at 1.39 eV in the region of QW absorption, and one at 1.43 eV in the region of GaAs absorption. These peaks may reflect the interplay between PVs coming from the buffer and surface fields. An increase in the SPV amplitude indicates the dominance of the signal from the buffer field; a decrease in the signal means that the PV from the surface region dominates.

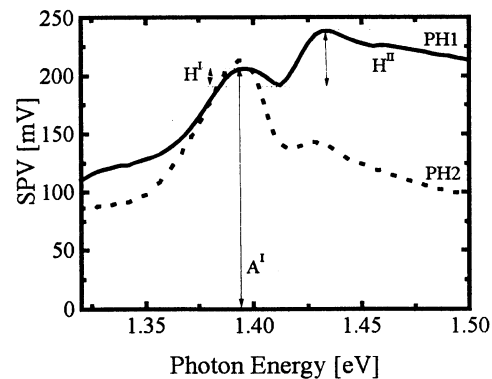


Fig.2. Surface photovoltage spectra of two PHEMT structures with a difference of 1×10^{12} cm $^{-2}$ in effective top delta doping level. Labels in the figure correspond to spectrum parameterization scheme (details in text).

Let us consider in more detail the SPV in the QW spectral region. Light absorption and generation of electron-hole pairs occur primarily in the QW. The PV is a result of carrier separation by electric fields. Thus, at the QW spectral region, escape of holes from the well is a crucial step for SPV formation. The escape rate of holes from the well depends on the hole barrier height. Depending on the electric field in the QW (F_{QW}), the hole barrier is not equal for the well-buffer (V_{buff}) and well-surface (V_{sur}) interfaces; as a result, the escape rate of carriers is also different. This is demonstrated in Fig. 3 where three possible F_{QW} directions are schematically shown.

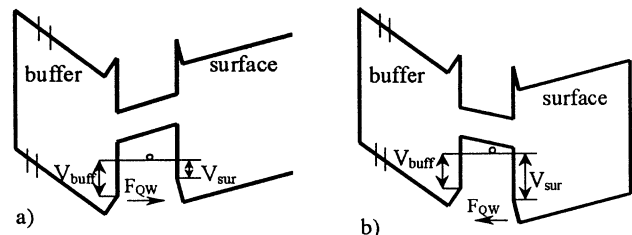


Fig.3. Schematic representation of the three possible band lineups in the QW region. a) $V_{sur} > V_{buff}$; b) $V_{buff} > V_{sur}$; direction is shown by arrow.

The PV magnitude is a complicated function of light absorption, hole escape rate from the well (when absorption takes place in the well), and the electric fields in any given region. To obtain further insight into these processes, numerical calculations have been performed using a simulation, which self-consistently solves the continuity equations for electrons and holes and the Poisson equation¹⁵. The results of such calculations based on the studied structure are shown in Fig. 4, where the SPV spectrum (solid line) together with the separate PV contributions of the buffer (dotted curve) and surface (dashed curve) are indicated.

Indeed, two peaks are observed in the calculated SPV spectrum (solid curve).

The first peak is dominated by absorption in the QW. Below a photon energy of 1.37 eV, the buffer (surface) PV increases (decreases) with increasing photon energy. The combination of these signals results in a monotonically increasing SPV. At 1.37 eV, the buffer PV saturates, while the PV at the surface layer continues to decrease monotonically and hence it becomes more dominant in the SPV spectrum. This is manifested as the first peak at 1.37 eV. A similar mechanism forms the second peak. Absorption in the GaAs buffer layer, which starts at 1.42 eV, leads to additional PV at this layer, followed by saturation at 1.425 eV. Since the surface layer PV decreases monotonically for the entire spectral range, a second maximum is obtained at 1.425 eV. Thus, the particular two-peaked curve is a result of the interplay of the two opposing PV signals.

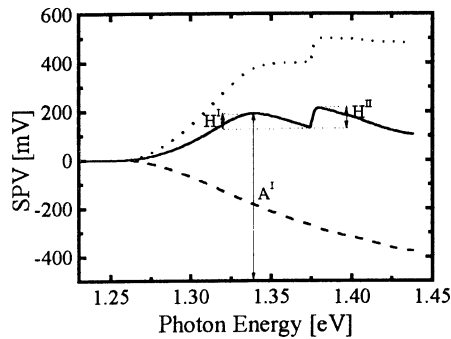


Fig.4. Calculated photovoltage signal from buffer (dotted curve) and surface layers (dashed curve) as a function of photon energy and the resultant SPV spectrum (solid curve). Labels in the figure correspond to spectrum parameterization scheme (details in text).

After establishing the relation between the physical mechanisms contributing to PV formation throughout the structure and the ensuing SPV, a simple empirical model has been developed in order to relate spectral features and structural parameters. This model is based on parameterization of the spectrum and a set of numerical simulations, which define the relation between structure and spectrum parameters. The parameterization of the spectrum is based on the amplitude of the first observed peak maxima A^I , and the magnitude of the two peaks with respect to the valley between them (H^I , and H^{II} , respectively). (See Fig. 2).

CORRELATION BETWEEN STRUCTURAL PARAMETERS AND SPECTRAL FEATURES.

The modeling was done by altering structure parameters in the simulation and following the changes in spectrum parameters. The light intensity in the simulation was assumed constant throughout the spectral range. The delta doping levels (denoted by δ_{top} and δ_{bot} for the top and bottom delta-doped layers, respectively) and the charge density at the external surface, Q_{sur} , were found to dominate the SPV

spectrum. The buffer/substrate interface charge density, Q_{int} , was not shown to significantly affect the spectrum. This is because the thick buffer layer reduces the effect of Q_{int} on the electric fields in the QW vicinity. Indeed, it is these structural parameters which determine the charge distribution and electric fields in the structure. Note that the energy position of the spectra features is only weakly dependent on these structure parameters.

Our analysis predicts a simple linear relation between the change in a specific structure parameter, ΔS_i and the corresponding change in spectral parameter, ΔA^J . Thus, a general formulation of the desired correlation may be represented by:

$$\Delta A^J = \sum_i C_i^J \cdot \Delta S_i \quad (1)$$

where C_i^J are the correlation coefficients, whose calculated average values are presented in table I. This simple model was found to be applicable for a wide range of structural parameters: $\delta_{top} \in [3-6 \times 10^{12} \text{ cm}^{-2}]$; $\delta_{bot} \in [0.4-1.5 \times 10^{12} \text{ cm}^{-2}]$; and $Q_{sur} \in [0.4-2 \times 10^{12} \text{ cm}^{-2}]$. It is important to note that this model is defined for a given light intensity. Altering the light intensity may significantly change the spectrum shape, therefore, it is important to keep the same light intensity throughout the measurement.

TABLE I
CORRELATION COEFFICIENTS BETWEEN STRUCTURAL PARAMETERS AND SPECTRAL FEATURES (SHOWN IN FIG. 4)

	$C\delta_{top}$ mV/10 ¹² cm ⁻²	$C\delta_{bot}$ mV/10 ¹² cm ⁻²	CQ_{sur} mV/10 ¹² cm ⁻²
A^I	110	-270	-70
H^I	30	-200	0
H^{II}	0	85	-10

Several observations on the correlation between structure and spectrum parameters can be made. H^{II} is practically sensitive only to δ_{bot} . This is because H^{II} reflects the spectral range, where most of the absorption takes place in the GaAs buffer. Therefore, the PV mostly depends on F_B , which in turn is dominated by δ_{bot} , as indicated by our simulations. H^I is affected by both delta-doped layers, while the effect of Q_{sur} is minor. This reflects the strong interplay between photovoltage from surface and buffer layers, as suggested above.

The presented model may be effectively used for inspecting variations in a structure parameter of a specific structure with respect to a reference one. Let us consider several examples. In the first example, two PHEMT structures labeled PH1 and PH2 are compared. The main difference between two structures is the top delta doping concentration ($\sim 10^{12} \text{ cm}^{-2}$). Differences in the top delta doping results in different carrier sheet density. Therefore, we expect the top delta doping to affect the SPV spectrum.

According to Table I, the main differences are expected in A^I and H^I values, while H^{II} value is expected to be the same. Fig. 2 shows the PH1 and PH2 SPV spectra.

Taking ΔA and ΔH values from the experimental data and substituting it to equation (1) allows to evaluate $\Delta\delta_{bot}$, $\Delta\delta_{top}$ and ΔQ_{sur} . Table II summarizes the results of the experimental spectral parameters and structural parameters evaluated from the parameterization analysis.

TABLE II
THE DIFFERENCES IN THE SPECTRAL PARAMETERS AND IN THE EVALUATED STRUCTURAL PARAMETERS FOR PH1 AND PH2 STRUCTURES.

ΔA^I [mV]	-7
ΔH^I [mV]	-62
ΔH^{II} [mV]	41
$\Delta\delta_{bot}$ [$\times 10^{12}$ cm $^{-2}$]	0.5
$\Delta\delta_{top}$ [$\times 10^{12}$ cm $^{-2}$]	1.3
ΔQ_{sur} [$\times 10^{12}$ cm $^{-2}$]	-0.2

Indeed, the difference in δ_{top} agrees with the nominal value to within 30%, which is the estimated relative error. The differences in other parameters are much smaller. Thus, SPS may be successfully applied to monitoring different growth procedures.

As a second example, the methodology was applied to monitoring surface treatments. Fig. 5 shows SPV spectra of sample with different surface conditions.

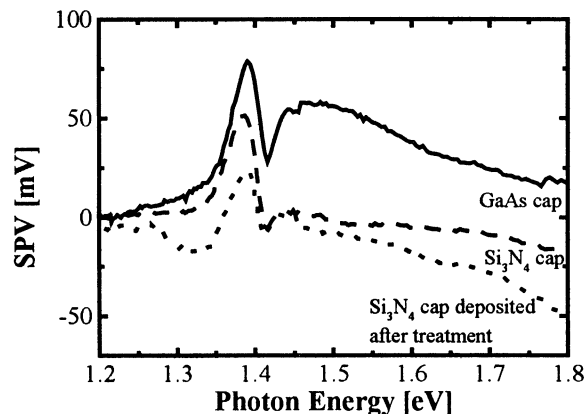


Fig.5. SPV spectra of the PHEMT sample with different surface conditions: solid line –GaAs cap; dashed line- with Si $_3$ N $_4$ cap layer; dots- with Si $_3$ N $_4$ cap layer deposited after plasma pretreatment.

As it may be expected, the change in the surface conditions may be monitored by change in amplitude of the SPV signal at first peak, i.e. A^I . The pretreatment by NH $_3$ 5%+N $_2$ plasma induces negative charge, of $\Delta Q_{sur} \sim 0.6 \times 10^{12}$ cm $^{-2}$, at semiconductor/nitride interface, compared to the standard nitride deposition process. This may be

related to effect of hydrogen radical deactivation of impurities at elevated temperatures.

CONCLUSIONS

In conclusion, the SPV spectra have been shown to be critically dependent on the particular electric field distribution at the buffer and surface layers of PHEMT structures. We have used SPS for developing an effective methodology for PHEMT structure analysis. Two examples demonstrate the capability of the methodology to characterize different process steps and surface treatments.

REFERENCES

- [1] M.Wojtowicz, D. Pascua, A.C. Han, T.R. Block, D.C. Streit, J. Cryst. Growth, **175**, 930 (1997)
- [2] Wu-Lu, J.H. Lee, K. Prasad, Geok-Ing-Ng, P. Lidstrom, J. Phys. D (Appl. Phys.) **31**, 159 (1998).
- [3] Y. Yin, H. Qiang, D. Yan, F.H. Pollak T.F. Noble, Semicond. Sci. Technol., **8**, 1599 (1993).
- [4] Y.S. Huang, W.D. Sun, L. Malikova, F.H. Pollak, I. Ferguson, H. Hou, Z.C. Feng, T. Ruan, E.B. Fantner, Appl. Phys. Lett., **74**,1851 (1999).
- [5] Y. Yin, H. Qiang, D. Yan, F.H. Pollak T.F. Noble, Semicond. Sci. Technol., **8**, 1599 (1993).
- [6] D.Y. Lin, S.H. Liang, Y.S. Huang, K.K. Tiong, F.H. Pollak, K.R. Evans, J. Appl. Phys., **85**, 8235 (1999).
- [7] T.J. Rogers, J.M. Ballingall, M. Larsen, E.L. Hall, J. Vac. Sci. Technol. B, **13**, 777 (1995).
- [8] D.Y. Lin, Y.S. Huang, K.K. Tiong, F.H. Pollak, K.R. Evans, Semicond. Sci. Technol., **14**, 103 (1999).
- [9] L. Kronik and Y. Shapira, Surf. Sci. Rep., **37**, 1 (1999).
- [10] B. Mishori, M. Leibovitch, Y. Shapira, F. H. Pollak, D. C. Streit, and M. Wojtowicz, Appl. Phys. Lett., **73**, 650 (1998).
- [11] N. Bachrach-Ashkenasy, L. Kronik, Y. Shapira, Y. Rosenwaks, M. C. Hanna, M. Leibovitch, and P. Ram, Appl. Phys. Lett., **68**, 879, (1996).
- [12] L. Aigoui, F. H. Pollak, T. J. Petruzello, and K. Shahzad, Solid. Stat. Comm., **102**, 877 (1997).
- [13] N. Ashkenasy, M. Leibovitch, Y. Shapira, F. H. Pollak, T. Burnham and X. Wang, J. Appl. Phys. **83**, 1146 (1998).
- [14] N. Ashkenasy, M. Leibovitch, Y. Rosenwaks, Y. Shapira, K. W. J. Barnham, J. Nelson, and J. Barnes, J. Appl. Phys. **86**, 6902 (1999).
- [15] G. A. Ashkinasi, M.G. Leibovitch and M. Nathan, IEEE Trans., **ED-40**, 285 (1993).
- [16] P.C.Chao, M.Y.Kao, , IEEE Electron Device Lett, **V 15**, 151 (1994).